Electroporation and mass spectrometry

Kocurek, Klaudia; Havlikova, Jana; Buchan, Emma; Tanner, Andrew; May, Robin; Cooper, Helen

DOI:
10.1021/acs.analchem.9b04365

analytical chemistry

pubs.acs.org/ac

Article

Electroporation and Mass Spectrometry: A New Paradigm for In Situ Analysis of Intact Proteins Direct from Living Yeast Colonies

Klaudia I. Kocurek, Jana Havlikova, Emma Buchan, Andrew Tanner, Robin C. May, and Helen J. Cooper*

Cite This: *Anal. Chem.* 2020, 92, 2605−2611

Read Online

ACCESS | Metrics & More | Article Recommendations | Supporting Information

ABSTRACT: Yeasts constitute an oft-neglected class of pathogens among which the resistance to first-line treatments, attributed in part to mutations in efflux pumps, is rapidly emerging. Their thick, chitin-reinforced cell walls render cell lysis difficult, complicating their analysis and identification by methods routinely used for bacteria, including matrix-assisted laser desorption/ionization time-of-flight mass spectrometry (MALDI-TOF-MS). Liquid extraction surface analysis mass spectrometry (LESA-MS) has previously been applied to the analysis of intact proteins from Gram-positive and Gram-negative bacterial colonies sampled directly on solid nutrient media. To date, a similar analysis of yeast colonies has not proved possible. Here we demonstrate the rapid release of intact yeast proteins for LESA-MS by electroporation using a home-built high-voltage device designed to lyse cells grown in colonies on agar media. Detection and identification of previously inaccessible proteins from baker's yeast *Saccharomyces cerevisiae*, as well as two clinically relevant yeast species (*Candida glabrata* and *Cryptococcus neoformans*), is shown. The electroporation approach also has the potential to be translated to other mass spectrometric analysis techniques, including MALDI and various ambient ionization methods.

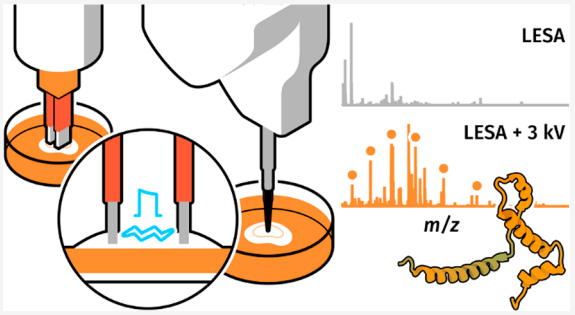

A growing number of ambient ionization mass spectrometry methods are available for the direct in situ analysis of large biomolecules, including intact proteins and protein complexes. Desorption electrospray ionization (DESI),[1] as well as a suite of liquid microjunction techniques such as nano-DESI,[2,3] liquid microjunction surface sampling probe (LMJ-SSP, commercialized as the Flowprobe),[4,5] and liquid extraction surface analysis (LESA)[6−9] have been coupled to mass spectrometry for the analysis of intact proteins directly from a variety of biological substrates.

LESA MS offers two advantages over the other ambient approaches. The discrete sampling mechanism, in contrast to the continuous flow of nano-DESI and the Flowprobe, ensures that no dilution of the analytes occurs, increasing sensitivity for proteins of low abundance. It also has the capability (thus far unique among ambient ionization methods) to lyse bacterial colonies directly on nutrient media and extract their cytosolic proteins,[10−13] an ability which could prove desirable for the identification and characterization of clinical isolates complementary to MALDI-TOF MS, the current gold standard.[14−17] MALDI-TOF MS-based identification of pathogens relies on the comparison of fingerprint protein mass spectra, consisting primarily of ribosomal and housekeeping proteins below 20 kDa, proteins which fall in the range observable by LESA-MS.[18,19] While optimization of the mode of sampling and solvent composition proved sufficient to enable the extraction of intact proteins from a variety of Gram-negative and Gram-positive bacterial species of clinical relevance, the application of a similar approach to yeast colonies was unsuccessful. Mass spectra generated from yeast colonies following sampling with harsh acetonitrile-based solvent systems were sparse and devoid of peaks attributable to proteins, indicating that lysis was not achieved. The most likely reason for this issue was the presence of a rigid, chitinous cell wall in yeasts. Existing protocols designed for MALDI-based workflows recommend extended centrifugation of yeast cultures in 70% formic acid followed by 100% acetonitrile to achieve protein extraction,[20] an approach which was not feasible for LESA of living colonies.

We proposed to resolve this challenge by electroporation, that is, cell permeation or lysis through application of high voltages. For biochemical purposes, electroporation is usually performed in suspension, whereas here it was adapted to the treatment of solid samples. The process is rapid (seconds) and introduces no additional chemical background into the sample; furthermore, it could potentially be coupled directly to the LESA apparatus to aid in automating the workflow. No commercial apparatus could, however, be identified which

Received: September 25, 2019
Accepted: January 10, 2020
Published: January 10, 2020

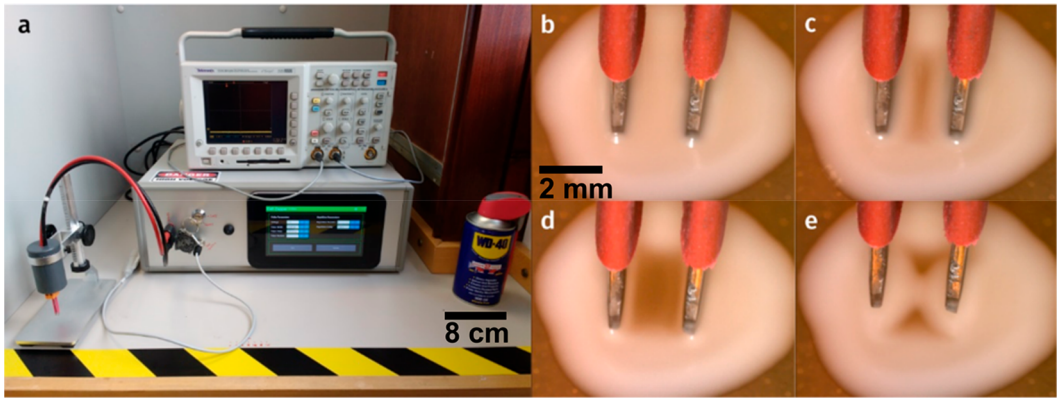

Figure 1. Overview of the electroporator and the electroporation process. a. The final device used in the study. The electrode assembly is seen on the left. b. Colony undergoing electroporation immediately following insertion of the electrodes; c. Following approximately seven pulses. d. Following delivery of 15 pulses over 15 s. e. Immediately following withdrawal of the electrodes.

would fulfill all the requirements for successfully lysing solid microbial samples directly on agar media. We thus designed and constructed a device in house. Described here is the general layout of the apparatus and its specifications. Parameters for lysis and protein extraction by LESA were optimized using *Saccharomyces cerevisiae* as a model system, followed by extraction and top-down identification of intact proteins (including cytosolic, nuclear, and mitochondrial species) in isolates of *Candida glabrata* and *Cryptococcus neoformans*. The two isolates were chosen for their role in a growing number of difficult-to-treat fungal infections. Over 30 proteins of multiple classes were confidently identified across the chosen species.

METHODS

Materials. Acetonitrile and HPLC-grade water were purchased from J.T. Baker, Deventer, Netherlands. Formic acid and powdered, premixed yeast extract peptone dextrose (YPD) broth were purchased from Sigma-Aldrich, Gillingham, UK. Bacteriological agar was purchased from VWR International, Leuven, Belgium. Donor plates of *Saccharomyces cerevisiae* BY4741 were provided by Dr Saverio Brogna at the University of Birmingham, UK. Donor plates of *Candida glabrata* (in-house strain) and *Cryptococcus neoformans* H99 were sourced from the Institute of Microbiology and Infection, University of Birmingham, UK.

Colonies of the three yeast species were inoculated from overnight liquid YPD cultures onto YPD agar plates (60 mm diameter) and incubated at 30 °C until the colonies reached a size suitable for sampling (approximately 5 mm diameter).

Electroporation Device. A photograph of the completed electroporator is provided in Figure 1a and a schematic is provided in Supporting Information (SI) Figure S1. For pulse delivery, stainless steel planar electrodes were installed in a detachable plug socket, allowing for easy cleaning and sterilization. The spacing between the electrodes was set to 2 mm to achieve the desired field strength of 15 kV/cm using a general-purpose power supply generating 3 kV. The electrode assembly was installed on a microscope stand to allow the electrodes to be lowered into the yeast colonies in a controlled manner. The device was controlled through custom software installed on a dedicated touchscreen interface based on the Raspberry Pi architecture. Further technical details of the apparatus are provided in the SI.

Cell Lysis. Plates containing colonies of interest were placed underneath the electrode assembly of the custom-built electroporation apparatus. The electrodes were lowered into the target colony; care was taken not to pierce the agar media below. Fifteen pulses (3 kV, corresponding to a field strength of 15 kV/cm), 20 μs in width and spaced 1 s apart, were delivered to each colony and monitored by oscilloscope (Textronics, Beaverton, OR). Following electroporation in batches, plates were stored at 4 °C until sampling (approximately 15 min to 3 h).

LESA. Sampling was carried out as described before[12] by use of a TriVersa NanoMate robotic pipet system (Advion, Ithaca, NY). Briefly, 3 μL of extraction solvent were withdrawn from a solvent well. The proportions of the solvent system (consisting of acetonitrile, water and formic acid) were 50:45:5; control and optimization experiments performed on *S. cerevisiae* used a milder 40:60:1 composition to minimize the contribution of the solvent to cell lysis. Two μL were dispensed onto the colony, between the two imprints left by the electrodes; the pipet tip was brought into contact with the colony surface during sampling. Following 15 s of extraction, 2.5 μL were reaspirated. The sample was subsequently infused into the mass spectrometer by nanoESI at 1.75 kV and 0.3 psi.

The total time of analysis for each plate, containing between three and seven yeast colonies, did not exceed 1 h. The effect of water evaporation from the agar substrate was minimized by cooling the sample plate to 4 °C during analysis and periodically adjusting the sampling height.

Mass Spectrometry. MS data acquisition was carried out by use of an Orbitrap Elite instrument (Thermo Scientific, Bremen, Germany) at a resolution of 120 000 at m/z 400, acquiring and coadding 10 microscans per scan. Full scan mass spectra in the m/z range from 600 to 2000 were acquired for a minimum of 5 min. Precursor ions were selected for fragmentation with an isolation window of 5 m/z. Collision-induced dissociation (CID) was performed in the ion trap with use of helium gas at a normalized collision energy of 35%; the fragments were detected in the Orbitrap. MS/MS spectra were recorded for 5 min. Each MS/MS scan comprised 30 coadded microscans. Automatic gain control targets were set to 1×10^6 charges for full scan mass spectra and 5×10^5 charges for MS/MS spectra.

Protein Identification. Top-down protein identification was performed with ProSightPC software, versions 3.0 to 4.1 alpha (Thermo Fisher Scientific, Bremen, Germany). MS/MS

https://dx.doi.org/10.1021/acs.analchem.9b04365
Anal. Chem. 2020, 92, 2605−2611

Table 1. Proteins Identified in Yeast by Electroporation-LESA-MS

m/z	charge	MW_{obs}	P-score	E-value	UniProt accession no.	ID
S. cerevisiae						
690.95	9	6248.52	8.6×10^{-19}	6.8×10^{-05}	P04650	L39
870.01	10	8690.05	9.1×10^{-23}	2.0×10^{-17}	P49167	L38
997.40	7	6974.73	8.1×10^{-14}	2.4×10^{-08}	A5Z2X5	YPR010C-A
1004.56	5	5017.78	3.5×10^{-60}	1.0×10^{-51}	P02994	EF1A
1042.05	12	12 492.50	3.1×10^{-33}	8.9×10^{-28}	Q08245	ZEO1
1046.52	7	7318.62	7.2×10^{-71}	2.1×10^{-62}	Q12497	FMP16
1069.78	5	5343.88	9.2×10^{-52}	2.7×10^{-43}	P38325	OM14
1086.59	6	7339.83	1.7×10^{-10}	6.8×10^{-05}	P0C5N0	YFR010W-A
1161.28	10	11 596.63	1.8×10^{-93}	4.7×10^{-88}	P22943	HSP12
1255.85	7	8778.89	2.4×10^{-38}	3.2×10^{-37}	P50263	SIP18
C. glabrata						
691.74	9	6213.58	1.7×10^{-20}	7.1×10^{-16}	B4UN51	L39-like protein
733.03	9	6584.26	2.9×10^{-9}	1.2×10^{-4}	Q6FWE3	S29
739.59	12	8858.06	1.8×10^{-14}	7.7×10^{-10}	Q6FXW9	L38-like protein
888.64	11	9758.93	1.7×10^{-37}	7.2×10^{-33}	Q6FMF8	S21
919.39	15	13 775.74	6.6×10^{-15}	2.8×10^{-10}	Q6FWM7	Histone H2A.1
955.38	7	6680.59	1.5×10^{-34}	9.5×10^{-24}	Q6FWE8	COX7A
1155.65	6	6923.84	1.8×10^{-13}	2.8×10^{-08}	B4UN07	COX7
1233.26	9	11 084.22	1.4×10^{-110}	4.7×10^{-106}	Q6FPF6	HSP12
1347.83	8	10 774.66	4.1×10^{-7}	1.7×10^{-02}	B4UN11	HMG box protein
1380.09	8	11 032.68	7.1×10^{-38}	7.0×10^{-35}	Q6FND5	Thioredoxin
C. neoformans						
692.85	9	6226.61	9.2×10^{-24}	3.3×10^{-19}	J9VPZ8	L39
741.42	5	3702.06	4.7×10^{-19}	4.7×10^{-19}	J9VMZ0	Histone H3 (C-term.)
877.05	9	7879.36	6.8×10^{-18}	2.2×10^{-13}	J9VPT7	S28
878.94	11	9657.23	9.4×10^{-14}	3.4×10^{-09}	J9VK09	F-type ATPase F
901.65	7	6304.49	2.0×10^{-41}	7.3×10^{-37}	J9VVE3	COX7A
960.35	9	8629.04	1.8×10^{-29}	5.8×10^{-25}	J9VUT1	CNAG_03143
968.97	7	6775.73	4.8×10^{-38}	1.7×10^{-33}	J9VST2	L29
1042.22	7	7285.49	1.5×10^{-54}	4.8×10^{-50}	J9VJQ8	CNAG_01446
1072.57	5	5357.80	3.6×10^{-73}	1.3×10^{-65}	J9W384	COX7C (C-term.)
1741.87	4	6960.46	6.8×10^{-32}	2.2×10^{-27}	J9VYN0	CNAG_04105

spectra were deconvoluted by the THRASH algorithm at a signal-to-noise ratio of 3. These were then matched against custom databases constructed for each species from full proteome data available via UniProt, using the Absolute Mass or the Biomarker mode as necessary (the latter aids the identification of truncated protein forms). Each database was constructed as a standard top-down database, taking into account the cleavage of initial methionines and N-terminal acetylation. Single nucleotide polymorphisms and all available posttranslational modifications were considered, with up to 13 features per sequence and a maximum mass of 70 kDa. For *S. cerevisiae*, the reference proteome of the ATCC 204508/S288c strain was used (UniProt ID UP000002311, 6049 protein entries, 403128 proteoforms). For *C. glabrata*, the only available reference proteome was used (UniProt ID UP000002428, 5200 protein entries, 42 226 proteoforms). For *C. neoformans*, the UniProt proteome corresponding to the H99 strain was used (UniProt ID UP000010091, 7430 protein entries, 32 270 proteoforms).

A broad absolute mass search was specified for each investigated species. Protein hits were considered within 2 kDa of the measured intact mass. Disulfide bridges were taken into account. The Δm mode, accounting for post-translational modifications or amino acid substitutions not present in the database, was active. All available post-translational modifications were taken into account. Fragment tolerance was set to ±15 ppm. Putative protein assignments were verified manually.

RESULTS AND DISCUSSION

Overview and Optimization of the Electroporation Device. A photograph of the completed electroporator is provided in Figure 1a. The parameters of the electroporation device were derived from fundamental research on electroporation conducted by Sale and Hamilton.[21] The electric field strengths required for the efficient lysis of some common microbial species were of particular importance; based on literature data, we determined that the device should be able to generate electric fields of 15 kV/cm, delivered as a variable number of square wave pulses whose width should be freely adjustable between 1 and 20 μs.

Notably, under the most vigorous lysis conditions tested during optimization (2−3 kV), colonies became visibly liquefied (Figure 1b−e). The matter between the electrodes became translucent as a large portion was drawn to the electrodes by surface tension; it would subsequently pool and set in its original position once the electrodes were removed. We attribute this behavior to the destruction of the cellular membranes and cell walls as well as, putatively, the matrix which provides structural support to the colony. Interestingly, no significant heating (>10 °C) is predicted to occur during delivery of the electric pulses, although these conclusions were

https://dx.doi.org/10.1021/acs.analchem.9b04365
Anal. Chem. 2020, 92, 2605−2611

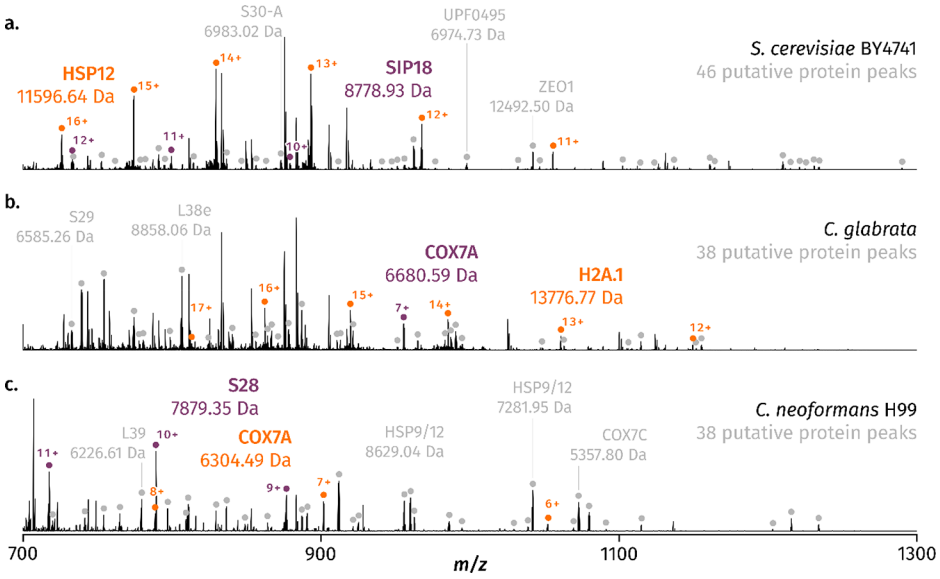

Figure 2. Representative mass spectra acquired by LESA MS following electroporation of colonies at optimized parameters. a. *S. cerevisiae*, b. *C. glabrata*, c. *C. neoformans*. Protein peaks (charge states 4+ and above) are marked with dots.

drawn based on literature data collected on cell suspensions rather than cell colonies on solid media.[21]

S. cerevisiae was used as a model system to determine optimum parameters for yeast electroporation prior to LESA-MS analysis. SI Figure S2a shows the LESA MS spectrum obtained in the absence of electroporation. No peaks corresponding to proteins were detected. Three electroporation variables were adjusted: the number of pulses, pulse width and voltage. Results are depicted in SI Figures S3−S5, respectively. According to early literature characterizing the process of electroporation on bacterial suspensions, these parameters were expected to have an impact on the percentage of lysed cells and therefore the efficiency of protein liberation. In particular, we expected a high total energy input to result in the greatest extent of lysis. A degree of variability was observed in the results which precluded the identification of exact threshold parameters at which protein liberation could be expected to occur. A number of factors may have contributed to this observation. First, the number of pulses successfully delivered to the colony varied as a result of arcing observed above the electroporated colony; this was limited to the first one to three pulses, following which electroporation proceeded normally. We found that the risk of arcing was minimized if the electrodes were placed carefully at a height not touching the conductive agar media underneath the colony. It is also worth noting that electroporation of colonies on agar media encounters challenges similar to electroporation of microbial suspensions. In particular, we found that the agar media should be kept salt-free as the presence of salts increases the risk of arcing and possible damage to the apparatus.

The positioning of the electrodes was manually controlled and thus the depth of their penetration into the colony (as well as their distance from the agar media) was not constant from sample to sample. Furthermore, the variations in colony morphology and their effect on LESA sampling have previously been documented and could also have an influence here. In light of these findings, subsequent work was carried out using the most disruptive settings tested here (15 pulses, 20 μs per pulse, at 3 kV) to maximize reliability. Liquefication of the colonies observed at these settings, while indicative of complete structural disintegration, resulted in an increased incidence of nozzle clogging during electrospray, most likely due to aspiration of colony debris. We found that this behavior could be alleviated by returning electroporated plates to cold storage for a short time (5−15 min) to allow the loose colony matter to resettle.

Protein Identification. Colonies of *S. cerevisiae* were subjected to a series of 15 pulses, 20 μs each with 1 s spacing, at 3 kV, as described above. Intact colonies grown on the same plate were used as control samples (see SI Figure S2a). A summary list of identified proteins is provided in Table 1. Peak assignments for all proteins identified in this section and corresponding supplementary tandem mass spectra are provided in the SI. We emphasize that the proteins selected for fragmentation are a representative sample, and that the number of protein identifications described below was not limited by the technical capability of the approach, that is, further identifications could be achieved with further MS/MS experiments. We also note that the molecular weights of the proteins identified are <15 kDa. This observation is typical for LESA MS conducted with denaturing solvents.[22]

In colonies subjected to electroporation, multiply charged peaks corresponding to protein were observed. Forty six peaks attributable to proteins were detected in the m/z 700−1300 region of the representative mass spectrum shown in Figure 2a. Mass spectra were dominated by the charge state distribution corresponding to the 12 kDa heat shock protein HSP12 (MW_{obs} = 11 596.64 Da), missing the initiator methionine and containing an acetylation on the N-terminal serine[23] (m/z 725.93 16+, 774.19 15+, 829.34 14+, 893.06 13+, 967.57 12+, 1055.44 11+, 1161.28 10+); the peaks at m/z 774.19 (15+), 893.06 (13+), and 1161.28 (10+) were isolated and fragmented for identification. The peak at m/z 1255.85 (7+; MW_{obs} = 8778.93 Da) was identified as the water deprivation stress response protein SIP18.[24] Eleven further peaks (690.95 9+, 870.01 10+, 874.38 8+, 997.40 7+, 1004.56 5+, 1042.05 12+, 1046.52 7+, 1047.10 7+, 1069.78 5+, 1086.59 6+, and 1113.38 5+) were fragmented, eight of which resulted in identification. In total, 10 proteins were successfully identified in *S. cerevisiae*.

https://dx.doi.org/10.1021/acs.analchem.9b04365
Anal. Chem. 2020, 92, 2605−2611

The peaks detected at m/z 690.95 (9+; MW_{obs} = 6248.52 Da) and 870.01 (10+; MW_{obs} = 8690.05 Da) were assigned to ribosomal proteins L39 and L38, respectively. Evidence for lysis of the mitochondrial membrane was provided by the identification of two mitochondrial proteins: The protein detected at m/z 1046.52 (7+; MW_{obs} = 7318.62 Da) was identified as the mitochondrial protein FMP16 involved in stress response to mild heat shock.[25] While manual sequence analysis listed in UniProt detected a 25 amino acid transit peptide at the N-terminus of the protein (a source for the assertion was not provided), the intact mass and fragmentation pattern recorded here are consistent with a 30-residue transit peptide (the N-terminal residue of the processed protein form is a proline). A truncated form of a second mitochondrial protein, OM14 (m/z 1069.78 5+, MW_{obs} = 5343.88 Da), a membrane protein involved in targeting of proteins to the mitochondrion, was also identified.

The high abundance of the 12 kDa heat shock protein at optimum growth conditions could be explained by its involvement in a number of other stress response mechanisms, including osmotic and oxidative stress.[23] Nevertheless, an attempt was made to reduce its intensity and reveal additional protein peaks by storing colonies of *S. cerevisiae* at 4 °C for 3 days prior to lysis and sampling. The colonies were subjected to the same electrical lysis regime as colonies sampled immediately following incubation. While the resultant mass spectra were dominated by singly charged species, peaks corresponding to HSP12 remained abundant, consistent with the role of HSP12 in stress response mechanisms other than heat shock.

Two peaks at m/z 772.99 5+ and 862.65 9+ were additionally observed; while they could also be detected at a lower abundance in colonies electroporated and sampled immediately following incubation, they were not previously selected for fragmentation. The two peaks could not be identified by the absolute mass search in ProSightPC 4.1 alpha. The biomarker search subsequently identified both peaks as two different fragments of the 12 kDa heat shock protein. The peak at m/z 772.99 5+ (MW_{obs} = 3859.90 Da) was identified as the N-terminal fragment of the protein containing the N-terminal acetylated serine; its sequence terminated at K36. The peak at m/z 862.65 9+ (MW_{obs} = 7754.78 Da) corresponded to the C-terminal fragment of the protein, residues A37 onward. Residues K36 and A37 are predicted to be located within an α-helix in the hinge region of the protein; NMR evidence suggests that the protein is intrinsically disordered in solution, but can adopt a four-helical conformation upon binding to lipids, which would be present in LESA yeast samples. The cleavage site was identified by PeptideCutter as a putative site for thermolysin and trypsin; neither protease is, however, endogenously expressed in yeast and thus the mechanism of cleavage remains unknown.

Colonies of *Candida glabrata* were subjected to a series of 15 or 20 pulses, 20 μs each with 1 s spacing, at 3 kV. Intact colonies grown on the same plate were used as controls, see SI Figure S2b. Several initial mass spectra were acquired following the delivery of 20 rather than 15 pulses as colonies of *Candida* were expected to require a higher energy to lyse than *S. cerevisiae* (approximately 12 kV/cm in suspension for 0% survival rate, versus 7 kV/cm for *S. cerevisiae*).[21]

The mass spectrum acquired from the control colony not subjected to electroporation contained peaks corresponding to a putative protein (m/z 1384.61 8+, 1230.88 9+, 1108.28 10+; MW_{obs} = 11068.82 Da). Each charge state was detected as a cluster of peaks spaced in approximately 18 Da increments. No other protein detected in *C. glabrata* exhibited a similar pattern. The 9+ charge state was isolated and fragmented, but the protein could not be identified. No other protein was observed in control colonies sampled immediately following incubation.

A representative mass spectrum acquired from a colony of *C. glabrata* subjected to electroporation, as compared to a control colony grown on the same plate, is shown in Figure 2b. Thirty-eight putative protein peaks were detected. Twenty-one peaks (m/z 691.74 9+, 733.03 9+, 739.59 12+, 754.18 8+, 769.23 10+, 806.74 11+, 853.64 13+, 870.95 6+, 888.64 11+, 919.39 15+, 924.78 12+, 951.20 9+, 951.22 8+, 955.38 7+, 990.13 7+, 1155.65 6+, 1220.01 8+, 1227.42 9+, 1233.26 9+, 1347.83 8+, and 1380.09 8+) were isolated and fragmented for identification. See Table 1. We note that the proteome of *C. glabrata* is currently poorly characterized; all protein assignments reported below were made on the basis of their homology to better-studied *S. cerevisiae* counterparts as listed in the UniProt database.

Crucially, the peak at m/z 919.39 (15+) was identified with high confidence as the histone protein H2A.1 (MW_{obs} = 13 775.74 Da) with its initiator methionine cleaved and the N-terminal serine acetylated, while m/z 769.23 (10+; MW_{obs} = 7682.26 Da) was identified as a fragment of histone H2A.1, inferred to exist in *C. glabrata* by homology. As histones are localized exclusively to chromatin packaged within the nucleus, the identification of a histone protein in colonies subjected to electric lysis constituted strong evidence that the cell membrane and the nuclear envelope were lysed by the application of the electric field. The protein detected at m/z 691.74 (9+, MW_{obs} = 6213.58 Da) was identified as the ribosomal constituent L39, not hitherto directly studied in *C. glabrata* but highly similar (>90% sequence identity) to its well-characterized homologue also observed here in *S. cerevisiae*; similarly, m/z 733.03 (9+, MW_{obs} = 6584.26 Da), m/z 739.59 (12+; also m/z 806.74, 11+, MW_{obs} = 8858.06 Da) and m/z 888.64 (11+; also 1220.01 8+, MW_{obs} = 9758.93 Da) were assigned to ribosomal components S29, L38 and S21, respectively, also identified based on their similarity in sequence and domain structure to *S. cerevisiae* homologues. The protein peaks at m/z 924.78 and 1233.26 (12+ and 9+, respectively; MW_{obs} = 11 084.22 Da) were identified as HSP12, a homologue of the 12 kDa heat shock protein previously identified in *S. cerevisiae*. Other identified proteins are listed in Table 1. The proteins detected at m/z 870.95 (6+; MW_{obs} = 5219.67 Da), and m/z 754.18 (8+) and 951.20 (9+; MW_{obs} = 6025.44 Da) could not be identified. The peak observed at m/z 951.22 (8+; MW_{obs} = 7601.76 Da) was tentatively assigned to CAGL0K03663g, but the quality of the tandem mass spectrum was insufficient to yield a highly confident identification.

In colonies stored for 3 days at 4 °C prior to electroporation and sampling, 37 protein peaks were detected in the m/z 700–1300 region. The 13+ charge state of the most abundant protein distribution (m/z 853.71, MW_{obs} = 11 084.22 Da) was isolated and confirmed as HSP12; six other charge states (m/z 740.09 15+, 792.81 14+, 924.77 12+, 1008.84 11+, 1109.63 10+, and 1226.97 9+) were also observed.

Colonies of *C. neoformans* H99 were subjected to 15 pulses of 20 μs at 3 kV. Intact colonies grown on the same plate were used as controls, see SI Figure S2c. While some multiply

https://dx.doi.org/10.1021/acs.analchem.9b04365
Anal. Chem. 2020, 92, 2605−2611

charged peaks, which may represent proteins, were found in the control mass spectrum, their abundance was extremely low and insufficient for isolation. A representative mass spectrum generated following electroporation from a colony of *C. neoformans* incubated for 48 h at 25 °C is shown in Figure 2c. Twelve peaks (692.85 9+, 717.68 11+, 741.42 5+, 877.05 9+, 878.94 11+, 901.65 7+, 960.35 9+, 968.97 7+, 1039.27 6+, 1042.22 7+, 1072.57 5+, and 1741.87 4+) were selected for identification. See Table 1. As was the case for *C. glabrata*, very little direct information on the proteome of *C. neoformans* is currently available and the protein identifications reported here rely entirely on the similarity of their sequence to homologues studied in other eukaryotes. Surprisingly, for H3 and L29 (see below), the closest well-studied homologues were found in plants.

Similarly to *C. glabrata*, evidence of histone proteins was detected in *C. neoformans*. The m/z 741.42 peak (5+; MW_{obs} = 3702.06 Da) was identified as a C-terminal fragment of histone H3. Three putative structural constituents of the ribosome, S28 (m/z 717.68, 11+ and 877.05, 9+; MW_{obs} = 7879.36 Da), L39 (m/z 692.85, 9+; also m/z 1039.27, 6+, MW_{obs} = 6226.61 Da) and L29 (m/z 968.97, 7+; MW_{obs} = 6775.73 Da) were identified; their database annotations have been inferred from homology and evidence for intact proteins has not hitherto been reported. m/z 960.35 (9+, MW_{obs} = 8629.04 Da) and m/z 1042.22 (7+; MW_{obs} = 7285.49 Da) were assigned to CNAG_03143 and CNAG_01446, respectively, two predicted, partially disordered proteins containing structural motifs which place them in the HSP9/HSP12 family; m/z 1741.87 (4+; MW_{obs} = 6960.46 Da) was identified as CNAG_04105, another partially disordered protein for which no functional data is currently available. The protein detected at m/z 860.05 (9+; MW_{obs} = 7731.35 Da) could not be identified.

CONCLUSION

The inclusion of electroporation in the LESA MS workflow as a means of lysing otherwise challenging cells was demonstrated to aid the extraction and identification of proteins in yeast colonies. These analytes could not previously be accessed by LESA MS. Based on current UniProt annotation, a significant proportion of the proteins reported here (that is, two in *S. cerevisiae* and all those described in *C. glabrata* and *C. neoformans*) have never been observed in their intact form by other techniques. Among those, the existence of two proteins (CAGL0K03663g in *C. glabrata* and CNAG_04105 in *C. neoformans*) was only hitherto predicted based on genomic data; they cannot be assigned to any known protein family based on their primary sequence and thus their function remains entirely unknown. These results show great promise for the identification and characterization of not only yeasts, which are in themselves a large class of clinically relevant organisms known to challenge current approaches, but also other microbes which do not easily yield to lysis by solvent, such as certain Gram-positive bacteria. While some species may require electric field strengths higher than those reported here for efficient lysis, 30 kV/cm (the limit at which air breakdown occurs) could be achieved by reducing the distance between the electrodes to 1 mm, which would still generate a sufficiently large area for subsequent LESA sampling. Furthermore, lysis by electroporation reduces the reliance of LESA on chemical lysis during sampling, affording greater flexibility in the choice of extraction solvent. We envisage that this combination may allow access to a greater variety of potentially interesting analytes, particularly those intolerant of the harsh chemical conditions otherwise required to rupture microbial cells.

ASSOCIATED CONTENT

Supporting Information

The Supporting Information is available free of charge at https://pubs.acs.org/doi/10.1021/acs.analchem.9b04365.

SI1. Technical details of the electroporation device. SI2. Control mass spectra acquired prior to the inclusion of electroporation in the workflow. SI3. Optimisation of electroporation parameters. SI4. ProSightPC peak assignments and supplementary mass spectra of all proteins identified in this study (PDF)

AUTHOR INFORMATION

Corresponding Author

Helen J. Cooper − *School of Biosciences, University of Birmingham, Birmingham B15 2TT, U.K.*; orcid.org/0000-0003-4590-9384; Email: h.j.cooper@bham.ac.uk

Authors

Klaudia I. Kocurek − *School of Biosciences, University of Birmingham, Birmingham B15 2TT, U.K.*

Jana Havlikova − *School of Biosciences, University of Birmingham, Birmingham B15 2TT, U.K.*

Emma Buchan − *School of Biosciences, University of Birmingham, Birmingham B15 2TT, U.K.*

Andrew Tanner − *School of Biosciences, University of Birmingham, Birmingham B15 2TT, U.K.*

Robin C. May − *Institute of Microbiology and Infection, University of Birmingham, Birmingham B15 2TT, U.K.*

Complete contact information is available at: https://pubs.acs.org/10.1021/acs.analchem.9b04365

Notes

The authors declare no competing financial interest.

ACKNOWLEDGMENTS

H.J.C. is an EPSRC Established Career Fellow (EP/L023490/1 and EP/S002979/1). K.I.K. was in receipt of an EPSRC studentship in collaboration with the National Physical Laboratory. J.H. and E.B. are funded by the EPSRC Physical Sciences for Health Doctoral Training Centre (EP/L016346/1). R.C.M was supported by project MitoFun, funded by the European Research Council under the European Union's Seventh Framework Programme (FP/2007-2013)/ERC Grant Agreement No. 614562 and by a Wolfson Research Merit Award from the Royal Society. The Advion TriVersa NanoMate and Thermo Fisher Orbitrap Elite mass spectrometer used in this research were funded through Birmingham Science City Translational Medicine, Experimental Medicine Network of Excellence Project with support from Advantage West Midlands. Supplementary data supporting this research are openly available from the University of Birmingham data archive at DOI: 10.25500/edata.bham.00000413.

REFERENCES

(1) Garza, K. Y.; Feider, C. L.; Klein, D. R.; Rosenberg, J. A.; Brodbelt, J. S.; Eberlin, L. S. *Anal. Chem.* **2018**, *90* (13), 7785−7789.

(2) Hsu, C. C.; White, N. M.; Hayashi, M.; Lin, E. C.; Poon, T.; Banerjee, I.; Chen, J.; Pfaff, S. L.; Macagno, E. R.; Dorrestein, P. C. *Proc. Natl. Acad. Sci. U. S. A.* **2013**, *110* (37), 14855−14860.
(3) Hsu, C. C.; Chou, P. T.; Zare, R. N. *Anal. Chem.* **2015**, *87* (22), 11171−11175.
(4) Griffiths, R. L.; Randall, E. C.; Race, A. M.; Bunch, J.; Cooper, H. J. *Anal. Chem.* **2017**, *89* (11), 5684−5688.
(5) Feider, C. L.; Elizondo, N.; Eberlin, L. S. *Anal. Chem.* **2016**, *88* (23), 11533−11541.
(6) Griffiths, R. L.; Cooper, H. J. *Anal. Chem.* **2016**, *88* (1), 606−609.
(7) Griffiths, R. L.; Sisley, E. K.; Lopez-Clavijo, A. F.; Simmonds, A. L.; Styles, I. B.; Cooper, H. J. *Int. J. Mass Spectrom.* **2017**, *437*, 23−29.
(8) Edwards, R. L.; Creese, A. J.; Baumert, M.; Griffiths, P.; Bunch, J.; Cooper, H. J. *Anal. Chem.* **2011**, *83* (6), 2265−2270.
(9) Edwards, R. L.; Griffiths, P.; Bunch, J.; Cooper, H. J. *J. Am. Soc. Mass Spectrom.* **2012**, *23* (11), 1921−1930.
(10) Randall, E. C.; Bunch, J.; Cooper, H. J. *Anal. Chem.* **2014**, *86* (21), 10504−10510.
(11) Sarsby, J.; Griffiths, R. L.; Race, A. M.; Bunch, J.; Randall, E. C.; Creese, A. J.; Cooper, H. J. *Anal. Chem.* **2015**, *87* (13), 6794−6800.
(12) Kocurek, K. I.; Stones, L.; Bunch, J.; May, R. C.; Cooper, H. J. *J. Am. Soc. Mass Spectrom.* **2017**, *28* (10), 2066−2077.
(13) Kocurek, K. I.; May, R. C.; Cooper, H. J. *Anal. Chem.* **2019**, *91* (7), 4755−4761.
(14) Singhal, N.; Kumar, M.; Kanaujia, P. K.; Virdi, J. S. *Front. Microbiol.* **2015**, *6*, 16.
(15) Wieser, A.; Schubert, S. *TrAC, Trends Anal. Chem.* **2016**, *84*, 80−87.
(16) Fagerquist, C. K. *Expert Rev. Proteomics* **2017**, *14* (1), 97−107.
(17) Angeletti, S. *J. Microbiol. Methods* **2017**, *138*, 20−29.
(18) Claydon, M. A.; Davey, S. N.; EdwardsJones, V.; Gordon, D. B. *Nat. Biotechnol.* **1996**, *14* (11), 1584−1586.
(19) Holland, R. D.; Wilkes, J. G.; Rafii, F.; Sutherland, J. B.; Persons, C. C.; Voorhees, K. J.; Lay, J. O. *Rapid Commun. Mass Spectrom.* **1996**, *10* (10), 1227−1232.
(20) Cassagne, C.; Cella, A. L.; Suchon, P.; Normand, A. C.; Ranque, S.; Piarroux, R. *Med. Mycol.* **2013**, *51* (4), 371−377.
(21) Sale, A. J. H.; Hamilton, W. A. *Biochim. Biophys. Acta, Gen. Subj.* **1967**, *148* (3), 781.
(22) Griffiths, R. L.; Konijnenberg, A.; Viner, R.; Cooper, H. J. *Anal. Chem.* **2019**, *91* (14), 9330−9330.
(23) Welker, S.; Rudolph, B.; Frenzel, E.; Hagn, F.; Liebisch, G.; Schmitz, G.; Scheuring, J.; Kerth, A.; Blume, A.; Weinkauf, S.; Haslbeck, M.; Kessler, H.; Buchner, J. *Mol. Cell* **2010**, *39* (4), 507−520.
(24) Dang, N. X.; Hincha, D. K. *Cryobiology* **2011**, *62* (3), 188−193.
(25) Sakaki, K.; Tashiro, K.; Kuhara, S.; Mihara, K. *J. Biochem.* **2003**, *134* (3), 373−384.

https://dx.doi.org/10.1021/acs.analchem.9b04365
Anal. Chem. 2020, 92, 2605−2611